Design of a Compact 6-DOF Haptic Device to Use Parallel Mechanisms

Masaru Uchiyama[1], Yuichi Tsumaki[2], and Woo-Keun Yoon[3]

[1] Department of Aerospace Engineering, Tohoku University
uchiyama@space.mech.tohoku.ac.jp
[2] Department of Intelligent Machines and System Engineering, Hirosaki University
tsumaki@cc.hirosaki-u.ac.jp
[3] Intelligent Systems Research Institute, National Institute of Advanced Industrial Science and Technology (AIST) wk.yoon@aist.go.jp

Summary. We present design of a compact haptic device in which parallel mechanisms are utilized. The design realizes a large workspace of orientational motion in a compact volume of the device. The device is a parallel-serial mechanism consisting of a modified DELTA mechanism for translational motion and a spatial five-bar gimbal mechanism for orientational motion. We derive an analytical model of stiffness for the modified DELTA mechanism which we utilize for the design of a stiff platform for translational motion. The model shows that the compliance matrix is a function of kinematic parameters as well as elastic parameters of each mechanical element. Configuration dependency of the compliance matrix is therefore an important point to be noticed.

1 Introduction

A device to make a bridge between human haptic sense and data space is called a haptic device. It displays the sense of touch to a human. It transfers human haptic sense in the real world to signals in data space. Those devices include a tactile display, a force/torque display, etc. A master arm in a master/slave system is a type of haptic device that displays force/torque information at a slave arm. This paper discusses on the design of such a haptic device of master arm type.

For a haptic device of master arm type, PHANTOM of SensAble Technologies, Inc. [1] is well known. But this has not sufficient force/torque capacity and is unable to display a very rigid feeling. A non-holonomic haptic device to display a rigid contact using a wheel has been proposed [2]. However, it is difficult to realize a haptic device of six DOF (Degrees Of Freedom). Fast six-DOF motion is realize by a haptic device of magnetic levitation type [3]. However, the workspace of the device is limited. A parallel wire system [4] may realize fast motion but requires a large place for itself.

To solve those problems, this paper proposes to apply parallel mechanisms to the design. The target is to realize a compact six-DOF device with large workspace for orientational motion and with capability of high-frequency motion. A compact six-DOF parallel mechanism like [5] may be used as a haptic device. However, the haptic device built by such a parallel mechanism only, will have limitation in orientational workspace. It is difficult to realize a large orientational workspace by such a parallel mechanism. A redundant parallel mechanism [6] may enlarge the workspace to some extent but need extra motors.

A stiff and light-weight mechanism is needed to increase the bandwidth of frequency response. For this purpose, a parallel mechanism is a good selection. Stiffness analysis of a parallel mechanism has been studied by, for example, Gosselin [7]. However, he considers only the stiffness of each actuator. Huang [8] proposed a method of stiffness analysis for a parallel mechanism, in which elastic components are considered. However, his analysis does not deal with bearings at free joints that are often used in the parallel mechanism.

We present a design of a compact haptic device in which parallel mechanisms are utilized and a large orientational workspace is realized in a compact volume of the device [9]. The device is a parallel-serial mechanism consisting of a modified DELTA mechanism for translational motion and a spatial five-bar gimbal mechanism for orientational motion. We derive an analytical model of stiffness for the modified DELTA mechanism to design a stiff platform for translational motion [10].

The paper is organized as follows: In Section 2, the design of a mechanism for the haptic device is presented. In Section 3, a model for stiffness analysis is derived, based on which the design is elaborated in Section 4 to yield a mechanism with well-balanced stiffness. The paper is concluded in Section 5

2 Synthesis of a Compact 6-DOF Mechanism

In this section, we present synthesis of a compact six-DOF mechanism for a haptic device of a master arm type. Design requirements and a six-DOF mechanism to meet the requirements are presented.

2.1 Design Requirements

Design requirements for a mechanism of the targeted haptic device are listed as follows:

1. Capability of six-DOF motion,
2. Capability of high-frequency motion,
3. Compact space for placing, and
4. Large workspace.

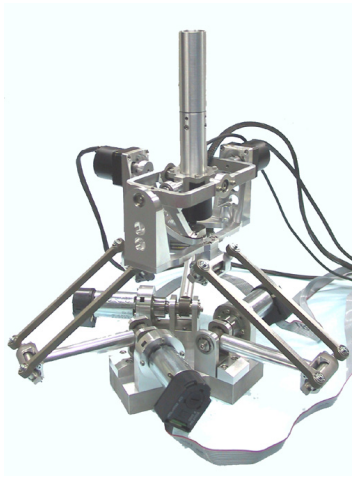

Fig. 1. Overview of the haptic device

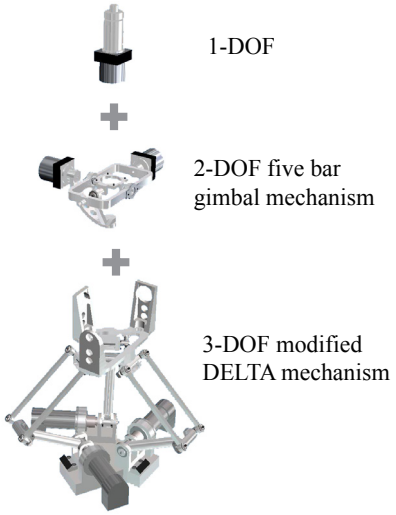

Fig. 2. DOF arrangement

To meet the requirements 1, 2, and 3, the parallel mechanism [11], [12] will be a good candidate. However, the requirement 4 for orientational motion will not be met by a parallel mechanism only, since orientational workspace of the parallel mechanism is usually very limited. In this paper, we solve the problem by applying two parallel mechanisms connected serially to translational motion and to orientation motion, separately.

2.2 A Compact 6-DOF Mechanism

The overview of the mechanism that we synthesize is shown in Figure 1. Architecture of the mechanism is shown in Figure 2, diagrammatically. As shown in the figure, the mechanism consists of three parts, two of which are parallel mechanisms, connected serially. The remaining one is a serial mechanism of one DOF. Thus, the mechanism is a parallel-serial mechanism.

The root of the mechanism is for three-DOF translational motion. Its overview is shown in Figure 3. It is a type of the DELTA mechanism invented by Clavel [13]. However, it is slightly different from the Clavel's DELTA. Difference is shown in Figure 4. The conventional DELTA uses ball joints to connect the rod to the arm on one end and to the traveling plate on the other, while the mechanism proposed in this paper uses ball bearings for those connections. We call this mechanism a modified DELTA mechanism. With the modification in the mechanism, we have larger movable range for the joints between arm and rod and between rod and traveling plate, respectively. This is shown in Figure 5. A similar mechanism has been proposed by Tsai [14].

The middle and the top parts of the mechanism are for orientational motion. The middle part is a five-bar gimbal mechanism [15] as shown in Figure 6.

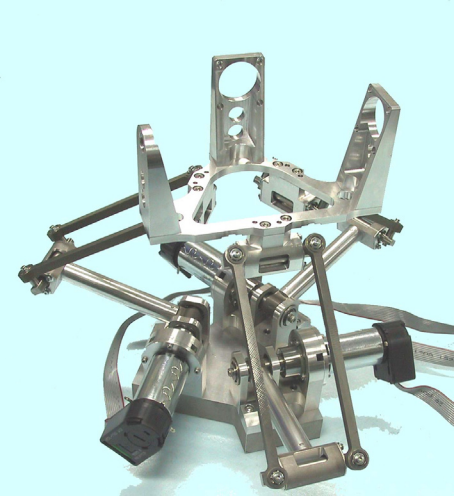

Fig. 3. The modified DELTA mechanism

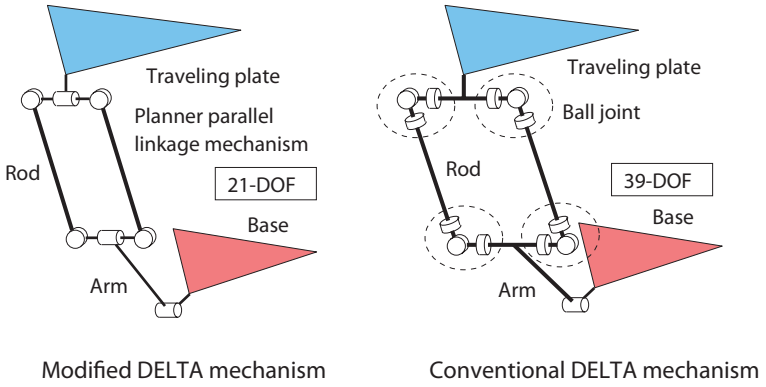

Fig. 4. Arrangement of DOF of the modified DELTA mechanism

This realizes two orientational motions, that is roll θ_r and pitch θ_p. Yaw motion θ_y is realized by the top part of the mechanism. An assembly drawing of the gimbal mechanism is shown in Figure 7. The axes for roll and pitch motions are supported by two bearings grounded on the rigid frame. It is noted that a parallel mechanism to implement the three orientational motions simultaneously has been proposed in [16], but we do not employ this mechanism because its movable range for yaw is small.

To meets the design requirements, the modified DELTA mechanism at the root has to be sufficiently stiff because it has to carry the mechanism for orientational motion. In the following sections we present procedure to design a stiff mechanism for this part.

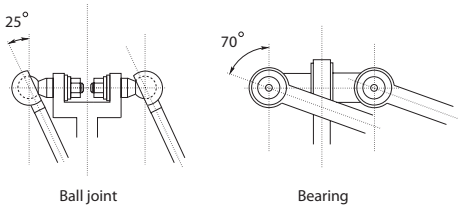

Fig. 5. Difference between limits of ball joint and bearing

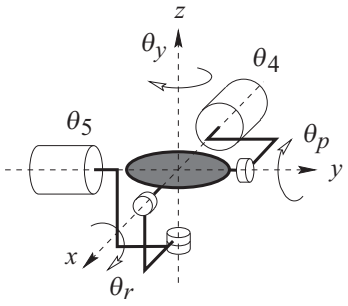

Fig. 6. The five-bar gimbal mechanism

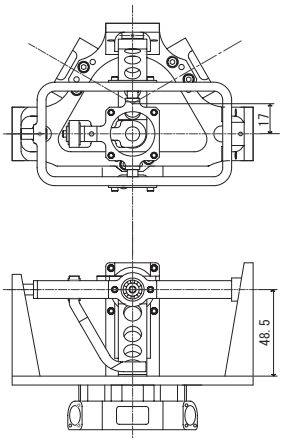

Fig. 7. An assembly drawing of the subsystem for orientational motion

3 Stiffness Analysis of the Modified DELTA Mechanism

In this section, we present a model for the analysis of stiffness of a parallel mechanism. Then, we apply this model to the modified DELTA mechanism presented in the previous section, and point out that the stiffness depends on the kinematic parameters, and therefore on the configuration of the mechanism, even when the same mechanical components are used.

3.1 A Stiffness Model of a Parallel Mechanism

A parallel mechanism is a closed-loop mechanism consisting of a base plate, a traveling plate and elementary chains that connect the two plates. Its stiffness is determined by the stiffness of each elementary chain. We assume the base and traveling plates are rigid. We begin with the analysis of the elementary chain and derive a compliance matrix of the target mechanism.

Tip Compliance of an Elementary Chain

The stiffness of each elementary chain is represented by its tip compliance [17], which we are going to derive here. Svinin and Uchiyama [18] studied the static compliant motion of a serial manipulator with elastic deformations in its structure. Let us suppose that the elementary chain consists of m elastic elements and n joints as shown in Figure 8. Forces and moments at each elastic element cause its elastic deformations of translation and rotation:

$$\boldsymbol{e}_i = \left[\delta_{xi} \ \delta_{yi} \ \delta_{zi} \ \phi_{xi} \ \phi_{yi} \ \phi_{zi} \right]^T \tag{1}$$

where $\boldsymbol{e}_i$ is an elastic deformation vector of the ith element. δ_{xi}, δ_{yi} and δ_{zi} are the translational deformations, and ϕ_{xi}, ϕ_{yi} and ϕ_{zi} are the orientational deformations, respectively. Assembling the all $\boldsymbol{e}_i$ for $i = 1, 2, \cdots, m$, we have an elastic deformation vector for the elementary chain:

$$\boldsymbol{e} = \left[\boldsymbol{e}_1^T \ \boldsymbol{e}_2^T \ \cdots \ \boldsymbol{e}_m^T \right]^T \tag{2}$$

which is determined by forces and moments on each element. If we suppose linear elasticity, we have

$$\boldsymbol{e} = \boldsymbol{C}_e \left[\boldsymbol{f}_1^T \ \boldsymbol{f}_2^T \ \cdots \ \boldsymbol{f}_m^T \right]^T \tag{3}$$

where

$$\boldsymbol{C}_e = \mathrm{diag} \left[\boldsymbol{C}_{e1} \ \boldsymbol{C}_{e2} \cdots \boldsymbol{C}_{em} \right] \tag{4}$$

is the compliance matrix of the all elastic elements, $\boldsymbol{C}_{ei}$ is the local compliance matrix of the ith elastic element, and $\boldsymbol{f}_i$ is the forces and moments acting on the ith element. The tip compliance matrix $\boldsymbol{C}_s$ of the elementary chain which relates the tip deformations of the elementary chain to the forces and moments applied at the tip is given by

$$\boldsymbol{C}_s = \boldsymbol{J}_e \left(\boldsymbol{\theta}, \boldsymbol{0} \right) \boldsymbol{C}_e \boldsymbol{J}_e^T \left(\boldsymbol{\theta}, \boldsymbol{0} \right) \tag{5}$$

assuming that the elastic deformation $\boldsymbol{e}$ is small, namely $\boldsymbol{e} = \boldsymbol{0}$ in $\boldsymbol{J}_e \left(\boldsymbol{\theta}, \boldsymbol{e} \right)$, where $\boldsymbol{J}_e \left(\boldsymbol{\theta}, \boldsymbol{e} \right)$ is the Jacobian matrix consisting of the Jacobian matrices for each elastic element defined by

$$\boldsymbol{J}_e \left(\boldsymbol{\theta}, \boldsymbol{e} \right) = \left[\boldsymbol{J}_{e1} \left(\boldsymbol{\theta}, \boldsymbol{e} \right) \boldsymbol{J}_{e2} \left(\boldsymbol{\theta}, \boldsymbol{e} \right) \cdots \boldsymbol{J}_{em} \left(\boldsymbol{\theta}, \boldsymbol{e} \right) \right] . \tag{6}$$

$\boldsymbol{J}_{ei} \left(\boldsymbol{\theta}, \boldsymbol{e} \right)$ is the Jacobian matrix for each elastic element. $\boldsymbol{J}_e \left(\boldsymbol{\theta}, \boldsymbol{e} \right)$ is a function of both $\boldsymbol{\theta}$ and $\boldsymbol{e}$. $\boldsymbol{\theta}$ is a joint angle vector.

Tip Compliance of a Parallel Mechanism

Using the compliance matrix of the elementary chain given by Equation (5) we derive a tip compliance matrix of the parallel mechanism shown in Figure 9.

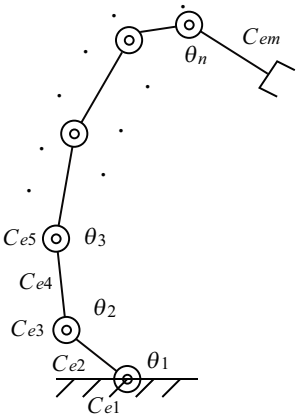

Fig. 8. A model of a serial mechanism

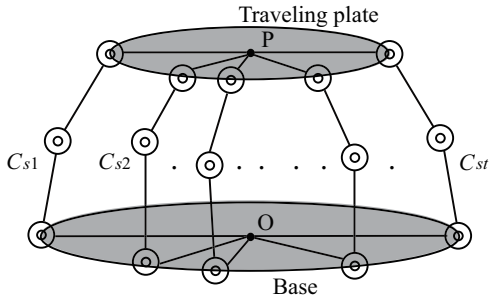

Fig. 9. A model of a parallel mechanism

This parallel mechanism consists of t elemental chains. The point O is the origin of the base plate and the point P on the traveling plate is the output point of the mechanism. Each elementary chain connects the points O and P. The tip compliance matrix of the parallel mechanism is given by

$$\boldsymbol{C}_p^{-1} = \boldsymbol{C}_{s1}^{-1} + \boldsymbol{C}_{s2}^{-1} + \cdots + \boldsymbol{C}_{st}^{-1} \tag{7}$$

where $\boldsymbol{C}_{sj}$ $(j = 1, 2, \cdots, t)$ is the compliance matrix of the jth elementary chain. It should be noted that the elastic deformations of both traveling plate and base plate are ignored.

Now, we have an equation to calculate the tip compliance matrix of the parallel mechanism. To calculate $\boldsymbol{C}_p$ by Equation (7), we need to have $\boldsymbol{C}_{ei}$ in Equation (4), that is a model for the ith elastic element. Typical elastic elements in a parallel mechanism are a link and a bearing. We present models for them in the following sections.

Modeling of a Link

Suppose that the ith elastic element is a link of a slender beam. Forces and moments on the beam cause elastic deformations. The relation between the forces and moments and the elastic deformations at the end of the beam is well known. It is expressed by

$$\boldsymbol{C}_{ei} = \begin{bmatrix} \frac{L^3}{3EI_x} & 0 & 0 & 0 & 0 & 0 \\ 0 & \frac{L^3}{3EI_y} & 0 & 0 & 0 & -\frac{L^2}{2EI_z} \\ 0 & 0 & \frac{L^3}{3EI_z} & 0 & \frac{L^2}{2EI_y} & 0 \\ 0 & 0 & 0 & \frac{L}{GI_p} & 0 & 0 \\ 0 & 0 & \frac{L^2}{2EI_z} & 0 & \frac{L}{EI_y} & 0 \\ 0 & -\frac{L^2}{2EI_y} & 0 & 0 & 0 & \frac{L}{EI_z} \end{bmatrix} \tag{8}$$

where L is the link length, E is the modulus of the longitudinal elasticity, G is the modulus of the transverse elasticity. I_x, I_y and I_z are the geometrical moments of inertia. I_p is the polar moment of inertia.

Modeling of a Bearing

A bearing is a machine element often used in the parallel mechanism. When the ith element is a bearing, the compliance matrix is given by

$$\boldsymbol{C}_{ei} = \begin{bmatrix} \frac{1}{k_a} & 0 & 0 & 0 & 0 & 0 \\ 0 & \frac{1}{k_r} & 0 & 0 & 0 & 0 \\ 0 & 0 & \frac{1}{k_r} & 0 & 0 & 0 \\ 0 & 0 & 0 & \Phi & 0 & 0 \\ 0 & 0 & 0 & 0 & \frac{1}{k_m} & 0 \\ 0 & 0 & 0 & 0 & 0 & \frac{1}{k_m} \end{bmatrix} \tag{9}$$

where k_a is the coefficient of elasticity in the axial direction, k_r is the coefficient of elasticity in the radial direction, $1/\Phi$ is the coefficient of rotational elasticity in the axial direction, and k_m is the coefficient of rotational elasticity in the radial direction. The direction of the x axis is chosen to be the rotation axis.

If the axial rotation is free, which is usually the case for a bearing, the coefficient of rotational elasticity $1/\Phi$ is nearly zero and Φ is close to infinity. However, if Φ is chosen close to infinity, the numerical calculation becomes unstable. Therefore, Φ should be chosen large enough but not close to infinity. In this paper, the value of 10^8 rad/Nm is used. This value is much larger than any other matrix elements.

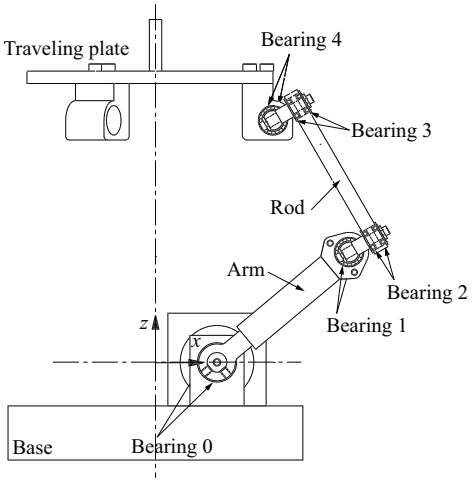

Fig. 10. An assembly drawing of the modified DELTA mechanism

3.2 Application of the Model to the Modified DELTA Mechanism

We apply the stiffness model derived in the previous section to the modified DELTA mechanism in order to obtain a compliance matrix for the mechanism. A schematic diagram of this mechanism is shown in Figure 10. This mechanism is made of a base, bearings 0, three arms, bearings 1 and 2, three rod parts, bearings 3 and 4 and a traveling plate. The output shaft of the motor is supported by the bearings 0. The rod part which consists of a planar parallel mechanism is made of the bearings 2, two parallel rods and the bearings 3 (see also Figures 3 and 4). The passive joints are equipped with conventional ball bearings that are mounted in pairs. We derive the compliance matrix for this mechanism, first deriving a model of the bearing pair, then a model of the rod part, and finally assembling those models.

Modeling of a Pair of Bearings

The connection between the rod part and the arm and between the rod part and the traveling plate is through a pair of bearings as shown in Figure 11. The coefficients of elasticity in the axial and radial directions of this part are obtained as those for a bearing multiplied by two. The coefficient of rotational elasticity in the axial direction is also obtained by the same way. However, the coefficient of rotational elasticity in the radial direction cannot be obtained simply by this way. This is obtained using a model of deformation shown in Figure 12. The moment M in the figure is obtained by

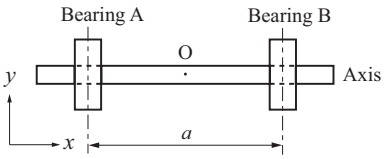

Fig. 11. A two bearing system

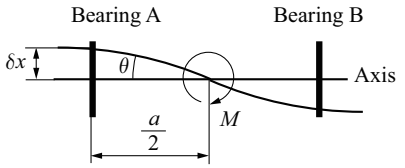

Fig. 12. Elastic deformation of the two bearing system

$$M = 2\left(k_m\theta + \frac{a}{2}\delta x k_r\right) = 2\left(k_m\theta + \frac{a}{2}\frac{a}{2}\theta k_r\right)$$
$$= 2\left\{k_m + \left(\frac{a}{2}\right)^2 k_r\right\}\theta \tag{10}$$

where δx is the elastic deformation in the radial direction, θ is the rotation angle, and a is the distance between the two bearings as shown in the figure. k_m and k_r are elastic coefficients. Therefore, we have the compliance matrix of the pair of bearings as follows:

$$\boldsymbol{C}_{ei} = \begin{bmatrix} \frac{1}{2k_a} & 0 & 0 & 0 & 0 & 0 \\ 0 & \frac{1}{2k_r} & 0 & 0 & 0 & 0 \\ 0 & 0 & \frac{1}{2k_r} & 0 & 0 & 0 \\ 0 & 0 & 0 & \frac{\Phi}{2} & 0 & 0 \\ 0 & 0 & 0 & 0 & \frac{1}{2\left\{k_m + \left(\frac{a}{2}\right)^2 k_r\right\}} & 0 \\ 0 & 0 & 0 & 0 & 0 & \frac{1}{2\left\{k_m + \left(\frac{a}{2}\right)^2 k_r\right\}} \end{bmatrix}. \tag{11}$$

Modeling of the Rod Part by a Parallel Mechanism

The rod part is made of a planar parallel mechanism. This parallel mechanism consists of two parallel rods and the bearings 2 and 3 as shown in Figure 10 (see also Figures 3 and 4). We consider the two rods (Rod L and R) separately as shown in Figure 13 and calculate the compliance matrix of each rod, first, and then, the compliance matrix of the whole rod system. According to Equation (4), the compliance matrices $\boldsymbol{C}_{eL}$ and $\boldsymbol{C}_{eR}$ for the rods L and R, respectively, shown in Figure 13, are given by

$$\boldsymbol{C}_{eL} = \mathrm{diag}\left[\boldsymbol{C}_{b2L}\ \boldsymbol{C}_{rL}\ \boldsymbol{C}_{b3L}\right] \tag{12}$$

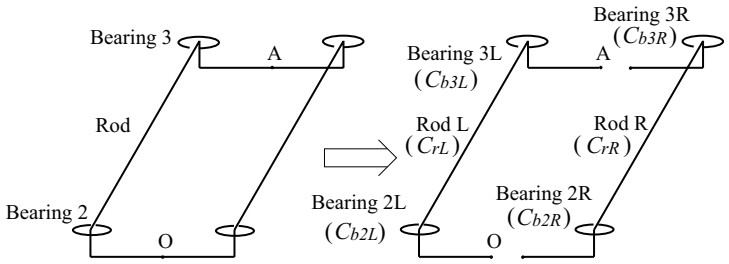

Fig. 13. Modeling of the rod part

and

$$\boldsymbol{C}_{eR} = \mathrm{diag}\left[\boldsymbol{C}_{b2R}\ \boldsymbol{C}_{rR}\ \boldsymbol{C}_{b3R}\right] \tag{13}$$

where $\boldsymbol{C}_{b2L}$, $\boldsymbol{C}_{b2R}$, $\boldsymbol{C}_{b3L}$ and $\boldsymbol{C}_{b3R}$ are the compliance matrices of the bearings 2L, 2R, 3L and 3R, respectively. $\boldsymbol{C}_{rL}$ and $\boldsymbol{C}_{rR}$ are the compliance matrices of the rods L and R, respectively. The Jacobian matrices $\boldsymbol{J}_{eL}(\boldsymbol{\theta}, \mathbf{0})$ and $\boldsymbol{J}_{eR}(\boldsymbol{\theta}, \mathbf{0})$ for the rods L and R are written as

$$\boldsymbol{J}_{eL}(\boldsymbol{\theta}, \mathbf{0}) = \left[\boldsymbol{J}_{b2L}(\boldsymbol{\theta}, \mathbf{0})\ \boldsymbol{J}_{rL}(\boldsymbol{\theta}, \mathbf{0})\ \boldsymbol{J}_{b3L}(\boldsymbol{\theta}, \mathbf{0})\right] \tag{14}$$

and

$$\boldsymbol{J}_{eR}(\boldsymbol{\theta}, \mathbf{0}) = \left[\boldsymbol{J}_{b2R}(\boldsymbol{\theta}, \mathbf{0})\ \boldsymbol{J}_{rR}(\boldsymbol{\theta}, \mathbf{0})\ \boldsymbol{J}_{b3R}(\boldsymbol{\theta}, \mathbf{0})\right]\ , \tag{15}$$

respectively, where $\boldsymbol{J}_{b2L}(\boldsymbol{\theta}, \mathbf{0})$, $\boldsymbol{J}_{b2R}(\boldsymbol{\theta}, \mathbf{0})$, $\boldsymbol{J}_{b3L}(\boldsymbol{\theta}, \mathbf{0})$ and $\boldsymbol{J}_{b3R}(\boldsymbol{\theta}, \mathbf{0})$ are the Jacobian matrices of the bearings 2L, 2R, 3L and 3R, respectively. $\boldsymbol{J}_{rL}(\boldsymbol{\theta}, \mathbf{0})$ and $\boldsymbol{J}_{rR}(\boldsymbol{\theta}, \mathbf{0})$ are the Jacobian matrices of the rods L and R, respectively. Therefore, the compliance matrices $\boldsymbol{C}_{\mathrm{rod}L}$ and $\boldsymbol{C}_{\mathrm{rod}R}$ for the rods L and R can be written as

$$\boldsymbol{C}_{\mathrm{rod}L} = \boldsymbol{J}_{eL}(\boldsymbol{\theta}, \mathbf{0})\,\boldsymbol{C}_{eL}\boldsymbol{J}_{eL}^{T}(\boldsymbol{\theta}, \mathbf{0}) \tag{16}$$

and

$$\boldsymbol{C}_{\mathrm{rod}R} = \boldsymbol{J}_{eR}(\boldsymbol{\theta}, \mathbf{0})\,\boldsymbol{C}_{eR}\,\boldsymbol{J}_{eR}^{T}(\boldsymbol{\theta}, \mathbf{0})\ , \tag{17}$$

respectively. Consequently, the compliance matrix of the rod part $\boldsymbol{C}_{2r3}$ is obtained as

$$\boldsymbol{C}_{2r3}^{-1} = \boldsymbol{C}_{\mathrm{rod}L}^{-1} + \boldsymbol{C}_{\mathrm{rod}R}^{-1}\ . \tag{18}$$

Stiffness of the Modified DELTA Mechanism

The modified DELTA mechanism consists of three elementary chains as shown in Figure 3. Each elementary chain is connected to the same traveling plate

which does not deform elastically. A point on the traveling plate can be a common tip for the three elementary chains. Therefore, we first derive the compliance matrices $\boldsymbol{C}_{sj}$ ($j = 1, 2, 3$) for the jth elementary chain using Equation (5). Then, using Equation (7), we obtain the compliance matrix $\boldsymbol{C}_p$ of the whole mechanism.

The compliance matrix $\boldsymbol{C}_{ej}$ ($j = 1, 2, 3$) defined by Equation (4) for each elementary chain is given by

$$\boldsymbol{C}_{ej} = \mathrm{diag}\left[\boldsymbol{C}_{b0j}\ \boldsymbol{C}_{aj}\ \boldsymbol{C}_{b1j}\ \boldsymbol{C}_{2r3j}\ \boldsymbol{C}_{b4j}\right] \tag{19}$$

where $\boldsymbol{C}_{b0j}$, $\boldsymbol{C}_{b1j}$ and $\boldsymbol{C}_{b4j}$ are the compliance matrices of the bearings 0, 1, and 4, respectively. $\boldsymbol{C}_{aj}$ is the compliance matrix of the arm. $\boldsymbol{C}_{2r3j}$ is the compliance matrix of the rod part. The Jacobian matrix $\boldsymbol{J}_{ej}(\boldsymbol{\theta}, \boldsymbol{0})$ is written as

$$\boldsymbol{J}_{ej}(\boldsymbol{\theta}, \boldsymbol{0}) = \left[\boldsymbol{J}_{b0j}(\boldsymbol{\theta}, \boldsymbol{0})\ \boldsymbol{J}_{aj}(\boldsymbol{\theta}, \boldsymbol{0})\ \boldsymbol{J}_{b1j}(\boldsymbol{\theta}, \boldsymbol{0})\ \boldsymbol{J}_{2r3j}(\boldsymbol{\theta}, \boldsymbol{0})\ \boldsymbol{J}_{b4j}(\boldsymbol{\theta}, \boldsymbol{0})\right] \tag{20}$$

where $\boldsymbol{J}_{b0j}(\boldsymbol{\theta}, \boldsymbol{0})$, $\boldsymbol{J}_{b1j}(\boldsymbol{\theta}, \boldsymbol{0})$ and $\boldsymbol{J}_{b4j}(\boldsymbol{\theta}, \boldsymbol{0})$ are the Jacobian matrices of the bearings 0, 1 and 4, respectively. $\boldsymbol{J}_{aj}(\boldsymbol{\theta}, \boldsymbol{0})$ is the Jacobian matrix of the arm. $\boldsymbol{J}_{2r3j}(\boldsymbol{\theta}, \boldsymbol{0})$ is the Jacobian matrix of the rod part. Therefore, the compliance matrix of the jth elementary chain $\boldsymbol{C}_{sj}$ is obtained by

$$\boldsymbol{C}_{sj} = \boldsymbol{J}_{ej}(\boldsymbol{\theta}, \boldsymbol{0})\,\boldsymbol{C}_{ej}\boldsymbol{J}_{ej}^{T}(\boldsymbol{\theta}, \boldsymbol{0})\ . \tag{21}$$

Combining the three matrices for the three elementary chains, the compliance matrix of the whole mechanism $\boldsymbol{C}_p$ is obtained by

$$\boldsymbol{C}_p^{-1} = \boldsymbol{C}_{s1}^{-1} + \boldsymbol{C}_{s2}^{-1} + \boldsymbol{C}_{s3}^{-1}\ . \tag{22}$$

As has been seen in the derivation, the compliance matrix $\boldsymbol{C}_p$ is a function of the joint angles $\boldsymbol{\theta}$, kinematic parameters of the structure, and elastic parameters of the components such as links, bearings, etc. The model obtained here in this section gives a tool to optimize those parameters through evaluation of the matrix $\boldsymbol{C}_p$.

4 Detailed Design of the Modified DELTA Mechanism

We discuss on the design of a modified DELTA mechanism utilizing the stiffness model derived in the previous section. Using this model we elaborate the stiffness of the modified DELTA mechanism to decide its parameters in details. We assume a specification that the workspace be around a sphere of 75 mm radius. The procedure of the design is listed as follows:

1. First, we consider the singular configuration to obtain a set of kinematic parameters and realize a singularity-free workspace. This part does not use the stiffness model but uses only a kinematic model.

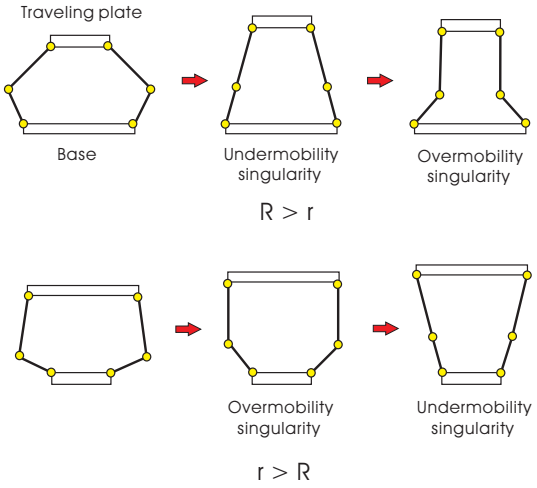

Fig. 14. Singular configurations

2. We discuss how each elastic element influences the tip stiffness and identify the elastic elements having a large influence on the reduction of the tip stiffness. Then, we use the results to improve the tip stiffness.
3. We discuss on kinematic parameters that influence on the tip stiffness and that may be used as a design index for a well-balanced tip stiffness.
4. Finally, we propose an index for the design of a modified DELTA mechanism and give a design example.

4.1 Singular configuration

Two types of singular configuration are considered. They are undermobility and overmobility singularities [12]. Figure 14 shows the two types of singularity for the modified DELTA mechanism, diagrammatically on a plane. This figure suggests that the case where the base radius R is equal to or larger than the traveling plate radius r be more recommendable than the case where $r > R$ because the former case does not have overmobility singularity in the workspace.

In the following discussion, we set both the traveling plate radius and the base radius equal to 40 mm. Also, since the workspace is given around a sphere of 75 mm radius, we set the sum of the arm length and of the rod length 220 mm, the minimum height 50 mm in order to avoid the undermobility, and the maximum height 200 mm in order to avoid the overmobility.

4.2 Parameters of the Modified DELTA Mechanism

Kinematic parameters of the modified DELTA mechanism are shown in Figure 15. Point O is the origin and point T is the tip position. L is the arm

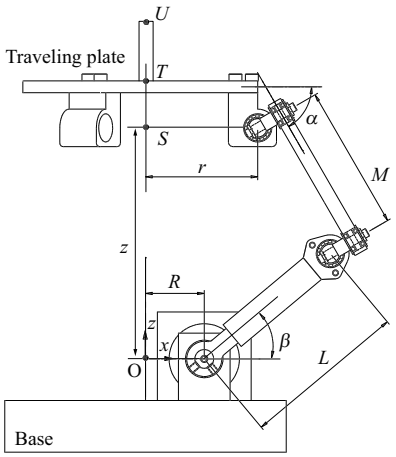

Fig. 15. Kinematic parameters of the modified DELTA mechanism

Table 1. Values of kinematic parameters

Parameter	[mm]
Rod length M	110
Arm length L	110
Base radius R	40
Traveling plate radius r	40

length, M is the rod length, R is the base radius, r is the traveling plate radius and z is the traveling plate height which is the distance between points O and S. Here, we deal with the case where the distance between points S and T is 15 mm, the distance between points T and U is 63.5 mm, and the distance between the two parallel rods at the rod part is 31 mm. The values of M, L, R, and r are given in Table 1.

It is assumed that the arms, rods, motor axes, bearings 0, 1, 2, 3 and 4 deform elastically. More specific details on the parts of the modified DELTA mechanism are given below:

- The arm is a hollow pole, made of A7075 material, with an internal diameter of 8 mm and an external diameter of 12 mm.
- The rod is a prismatic solid beam, made of SUS304 material, one side measure of which is 5 mm and the other 6 mm.
- Bearing 0 is an NSK model F688A. Bearings 1 and 4 are NSK model MR128.
- Bearings 2 and 3 are NSK model F684.
- The motor is a Maxon model A-max 26.

From the values of Table 1 and the elastic parameters of the above parts, we calculate the compliance matrices: $\boldsymbol{C}_{aj}$ for the arms, $\boldsymbol{C}_{rL}$ and $\boldsymbol{C}_{rR}$ for

the rods, $\boldsymbol{C}_{b0j}$, $\boldsymbol{C}_{b1j}$, $\boldsymbol{C}_{b2L}$, $\boldsymbol{C}_{b2R}$, $\boldsymbol{C}_{b3L}$, $\boldsymbol{C}_{b3R}$, and $\boldsymbol{C}_{b4j}$ for the bearings. All bearings are used in pairs.

The stiffness at the tip position (point U, see Figure 15) of the modified DELTA mechanism changes largely depending on the traveling plate position. Therefore, it is necessary to design the mechanism taking into consideration the tip stiffness at all points in the workspace. However, it is very difficult to evaluate all the 6×6 elements of the tip compliance matrix at all points. Therefore, we simplify the evaluation by limiting the point only in the z direction, with no motion in the (x, y) plane. In this case, $\boldsymbol{C}_p$ is given by

$$\boldsymbol{C}_p = \begin{bmatrix} A & 0 & 0 & 0 & B & 0 \\ 0 & A & 0 & -B & 0 & 0 \\ 0 & 0 & C & 0 & 0 & 0 \\ 0 & -B & 0 & D & 0 & 0 \\ B & 0 & 0 & 0 & D & 0 \\ 0 & 0 & 0 & 0 & 0 & E \end{bmatrix} \tag{23}$$

where A, B, C, D and E are non-zero elements determined by kinematic and elastic parameters.

It should be noted that the value of Φ for bearing 0 is measured directly in the real setup and made 0.0058 rad/Nm. In the bearing 0 a motor axis is inserted. Therefore, the compliance around this axis depends on the performance of the motor, control law, etc.

4.3 Influence of Each Elastic Element on the Tip Stiffness

Evaluating $\boldsymbol{C}_p$ in Equation (23) for each of the compliance matrices $\boldsymbol{C}_{aj}$ for the arms, $\boldsymbol{C}_{rL}$ and $\boldsymbol{C}_{rR}$ for the rods, $\boldsymbol{C}_{b0j}$, $\boldsymbol{C}_{b1j}$, $\boldsymbol{C}_{b2L}$, $\boldsymbol{C}_{b2R}$, $\boldsymbol{C}_{b3L}$, $\boldsymbol{C}_{b3R}$, and $\boldsymbol{C}_{b4j}$ for the bearings, with the rest of them being zero, we know influences of each elastic element on the tip compliance matrix. Through this numerical analysis we find that the influence on the element A and B of the bearings 2 and 3 is large, and we decrease the influence by replacing the bearings by ceramic bearings. Also, to decrease the influence of the arm on the elements C, D and E, we change the arm internal diameter to 10 mm and its external diameter to 14 mm. Like this way, the compliance matrix is improved.

4.4 Relation Between Tip Stiffness and α

The changes of the compliance matrix for the tip (point U) under elastic deformation of all the elements together (arms, rods, motor axes, bearings 0, 1, 2, 3, and 4) are shown in Figure 16, where α is the angle between the traveling plate and the rod as has been shown in Figure 15. According to Figure 16, when α increases, each of the elements A, B, C, D and E of Equation (23) changes as follows:

- The compliance in the direction of x- and y-axes (element A) increases.

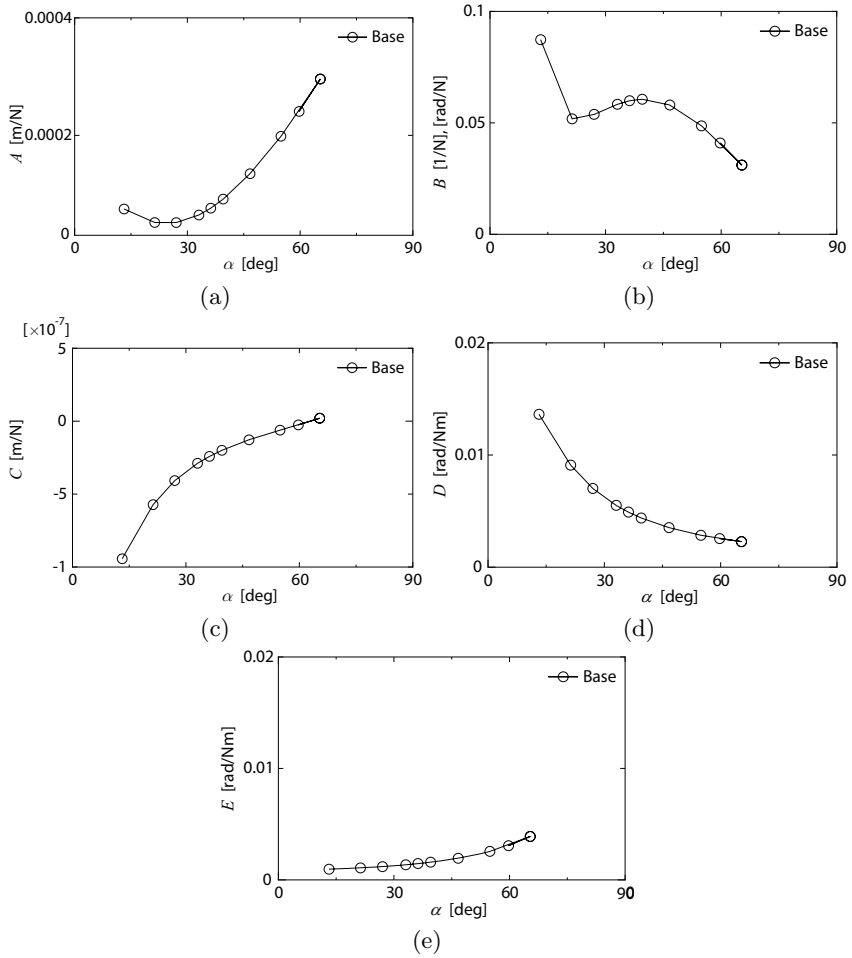

Fig. 16. Elements of the tip compliance matrix as a function of the parameter α

- The compliance of rotation around x- and y-axes against y and x forces, respectively, (element B) decreases for the most part of α, although it increases for a while at about 50 degrees.
- The compliance in the direction of x- and y-axes against y and x moments, respectively, (element B) changes in the same manner.
- The compliance in the direction of z-axis (element C) increases.
- The compliance of rotation around x- and y-axes (element D) decreases.
- The compliance of rotation around z-axis (element E) increases.

Therefore, in order to obtain a well-balanced stiffness, it is necessary to limit the value of α properly in the workspace.

4.5 A Design Index for the Modified DELTA Mechanism

From the above results, we find that the tip stiffness of the modified DELTA mechanism changes largely depending on the configuration, represented by the parameter α, even if elastic parameters are fixed. Therefore, we may use α as a design index. We should notice that the value of α depends on the base radius, the traveling plate radius, the arm length and the rod length. According to the results of numerical calculation, the value of α in the range from 40 to 70 degrees is best for realizing a well-balanced tip stiffness. If the value of α is outside this range, the stiffness of many elements decreases.

Based on the discussion, we decide that both the traveling plate and the base radii are 40 mm, the arm length is 93 mm and the rod length is 127 mm, in order to obtain a good balance of stiffness in the specified workspace (around a sphere of 75 mm radius).

5 Conclusions

We have presented a design of a compact haptic device in which parallel mechanisms are utilized and a large workspace of orientational motion is realized. The device is a parallel-serial mechanism consisting of a modified DELTA mechanism for translational motion and a spatial five-bar gimbal mechanism for orientational motion. We have derived an analytical model of stiffness for the modified DELTA mechanism, which we have utilized for the design of stiff platform for translational motion. The model shows that the compliance matrix is a function of kinematic parameters as well as elastic parameters of each element. Configuration dependency of the compliance matrix is an important point to be noticed. Key points newly proposed in the stiffness model are:

- Exploitation of stiffness analysis method for a flexible arm (manipulator) to obtain stiffness of the elementary chains in deriving the tip stiffness of the parallel mechanism.
- Modeling of the free motion around the axis of rotation in a bearing using a very small value of the elasticity coefficient.

We have obtained the following results regarding the design of the modified DELTA mechanism:

- The angle α can be a design index to optimize the stiffness of the modified DELTA mechanism.
- The stiffness of the bearings 2 and 3 should be sufficiently large.

From these results, we have found that α be restricted within the value between 40 to 70 degrees in order to obtain a well-balanced stiffness.

Future research will be directed to design of a more compact haptic device with higher frequency response using an actuator with faster response and with less friction.

References

1. Massie TH, Salisbury JK (1994) The PHANToM haptic interface: a device for probing virtual objects. In: Proc. 1994 ASME Int. Mechanical Engineering Exposition and Congress, Chicago, Illinois. pp 295–302
2. Colgate JE, Peshkin MA, Wannasuphoprasit W (1996) Nonholonomic haptic display. In: Proc. 1996 IEEE Int. Conf. on Robotics and Automation, Minneapolis, Minnesota. pp 539–544
3. Berkelman PJ, Hollis RL, Salcudean SE (1995) Interacting with virtual environments using a magnetic levitation haptic interface. In: Proc. IEEE/RSJ Int. Conf. on Intelligent Robots and Systems, Pittsburgh, Pennsylvania. pp 117–122
4. Hirata Y, Sato M (1992) 3-dimensional interface device for virtual workspace. In: Proc. IEEE/RSJ Int. Conf. on Intelligent Robots and Systems, Raleigh, North Carolina. pp 889–896
5. Inoue H, Tsusaka Y, Fukuizumi T (1986) Parallel manipulator. In: Faugeras O, Giralt G (eds) Robotics research, the third international symposium. The MIT Press. pp 321–327.
6. Hayward V (1995) Toward a seven axis haptic device. In: Proc. IEEE/RSJ Int. Conf. on Intelligent Robots and Systems, Pittsburgh, Pennsylvania. pp 133–139
7. Gosselin C (1990) Stiffness mapping for parallel manipulator. IEEE Trans. on Robotics and Automation 6:377–382
8. Huang T, Zhao X, Whitehouse DJ (2002) Stiffness estimation of a tripod-based parallel kinematic machine. IEEE Trans. on Robotics and Automation 18:50–58
9. Tsumaki Y, Naruse H, Nenchev DN, Uchiyama M (1998) Design of a compact 6-DOF haptic interface. In: Proc. 1998 IEEE Int. Conf. on Robotics and Automation, Leaven, Belgium. pp 2580–2585
10. Yoon WK, Suehiro T, Tsumaki Y, Uchiyama M (2004) Stiffness analysis and design of a compact modified delta parallel mechanism. ROBOTICA 22:463–475
11. Merlet JP (2000) Parallel robots. Kluwer Academic Publishers
12. Uchiyama M (1994) Structures and characteristics of parallel manipulators. Advanced Robotics 8:545–557
13. Clavel R (1988) DELTA, a fast robot with parallel geometry. In: Proc. 18th Int. Symp. on Industrial Robots, Lausanne, Switzerland. pp 91–100
14. Tsai LW (1995) Multi-degree-of-freedom mechanisms for machine tools and like. U.S. Patent No. 5656905
15. Ouerfelli M, Kumar V (1994) Optimization of a spherical five-bar parallel drive linkage. Trans. ASME, J. of Mechanical Design 116:166–173
16. Gosselin CM, Hamel JF (1994) Development and experimentation of a fast three-degree-of-freedom spherical parallel manipulator. In: Jamshidi M, Yuh J, Nguyen C, Lumia R (eds) Proc. First World Automation Congress, Maui, Hawaii. TSI Press. 2:229–234
17. Komatsu T, Uenohara M, Iikura S, Miura H, Shimoyama I (1990) Compliance control for a two-link flexible manipulator. Trans. JSME, Series C 56:2642–2648 (in Japanese)
18. Svinin MM, Uchiyama M (1994) Contribution to inverse kinematics of flexible robot arms. JSME Int. J., Series C: Dynamics, Control, Robotics, Design and Manufacturing 37:755–764